

# Paclitaxel Has a Reduced Toxicity Profile in Healthy Rats After Polymeric Micellar Nanoparticle Delivery

Jun Lu<sup>1-4,\*</sup>, Yuqing Lou<sup>1,\*</sup>, Yanwei Zhang<sup>1,\*</sup>, Runbo Zhong<sup>1</sup>, Wei Zhang<sup>1</sup>, Xueyan Zhang<sup>1</sup>, Huimin Wang<sup>1</sup>, Tianqing Chu<sup>1</sup>, Baohui Han<sup>1-3</sup>, Hua Zhong<sup>1,3</sup>

<sup>1</sup>Department of Pulmonary Medicine, Shanghai Chest Hospital, School of Medicine, Shanghai Jiao Tong University, Shanghai, People's Republic of China; <sup>2</sup>Shanghai Institute of Thoracic Oncology, Shanghai Chest Hospital, School of Medicine, Shanghai Jiao Tong University, Shanghai, People's Republic of China; <sup>3</sup>Translational Medical Research Platform for Thoracic Oncology, Shanghai Chest Hospital, School of Medicine, Shanghai Jiao Tong University, Shanghai, People's Republic of China; <sup>4</sup>Department of Bio-Bank, Shanghai Chest Hospital, School of Medicine, Shanghai Jiao Tong University, Shanghai, People's Republic of China

\*These authors contributed equally to this work

Correspondence: Baohui Han; Hua Zhong, Department of Pulmonary Medicine, Shanghai Chest Hospital, School of Medicine, Shanghai Jiao Tong University, Shanghai, 200030, People's Republic of China, Email xkyyhan@gmail.com; 18930858216@163.com; eddieong8@hotmail.com

**Background:** Nanocarrier platforms have been indicated to have great potential in clinical practice to treat non-small cell lung cancer (NSCLC). Our previous Phase III clinical study revealed that polymeric micellar paclitaxel (Pm-Pac) is safe and efficacious in advanced NSCLC patients. However, the histopathological-toxicological profile of Pm-Pac in mammals remains unclear.

**Methods:** We examined the Pm-Pac-induced antitumour effect in both A549/H226 cells and A549/H226-derived xenograft tumour models. And then, we evaluated the short-term and long-term toxicity induced by Pm-Pac in healthy Sprague–Dawley (SD) rats. The changes in body weight, survival, peripheral neuropathy, haematology, and histopathology were studied in SD rats administered Pm-Pac at different dosages.

**Results:** In the A549-derived xenograft tumour model, better therapeutic efficacy was observed in the Pm-Pac group than in the solvent-based paclitaxel (Sb-Pac) group when an equal dosage of paclitaxel was administered. Toxicity assessments in healthy SD rats indicated that Pm-Pac caused toxicity at an approximately 2- to 3-fold greater dose than Sb-Pac when examining animal body weight, survival, peripheral neuropathy, haematology, and histopathology. Interestingly, based on histopathological examinations, we found that Pm-Pac could significantly decrease the incidences of paclitaxel-induced brain and liver injury but could potentially increase the prevalence of paclitaxel-induced male genital system toxicity.

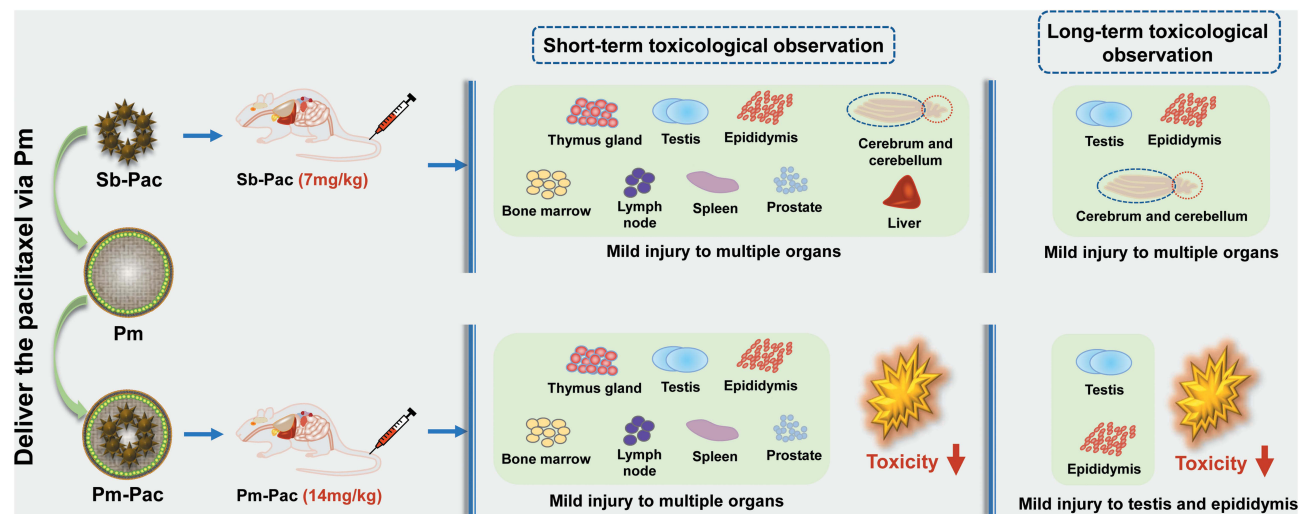
**Conclusion:** This study introduces the toxicological profile of the engineered nanoparticle Pm-Pac and provides a novel perspective on the Pm-Pac-induced histopathological-toxicological profile in a rat model.

**Keywords:** nanomedicine, polymeric micellar paclitaxel, NSCLC, toxicological profile

## Background

Non-small cell lung cancer (NSCLC) is a disease that causes one of the most malignant types of tumours and accounts for the vast majority of cancer deaths worldwide.<sup>1-4</sup> In the past few decades, the development of NSCLC treatments has greatly improved, and the overall survival (OS) of NSCLC patients has remarkably increased.<sup>4-6</sup> Currently, multiple therapeutic modalities (such as chemotherapy, antiangiogenic therapy, tyrosine kinase inhibitor (TKI) therapy, immunotherapy, and photodynamic therapy) are used in clinical practice.<sup>7,8</sup> However, chemotherapy still plays an important role as the cornerstone of NSCLC therapy.<sup>9,10</sup> Although novel therapeutic modalities, including immunotherapy, TKI therapy, and antiangiogenic therapy, have been developed, the objective response rate (ORR) will be enhanced significantly when these therapies are combined with chemotherapy.<sup>9,11-13</sup> Thus, a conundrum continues to preclude clinical practice; that is, although chemotherapy is the standard for NSCLC treatment, the main adverse event of therapy-induced toxicity remains a difficult challenge<sup>10,14</sup> that limits the dosages of chemotherapeutic drugs used clinically.

## Graphical Abstract



With the development of nanotechnology, multiple nanocarrier platforms have been used to improve anticancer drug delivery efficiency.<sup>14–17</sup> However, it is still debatable whether the delivery pattern of nanoparticle-enveloped chemotherapeutic drugs can reduce toxicity and improve efficacy.<sup>18</sup> Several studies have demonstrated that these nanocarriers play a potential role in reducing chemotherapy-induced toxicity.<sup>14,15</sup> However, only a few studies have demonstrated the effectiveness of nanocarriers in clinical trials.<sup>10,19–22</sup> Solvent-based paclitaxel (Sb-Pac) has been used to treat NSCLC clinically in recent decades. However, Sb-Pac-induced toxicity has limited increasing the dosage in clinical practice. Our previous study reported that polymeric micelles (Pm) nanoparticles are among the few paclitaxel nanocarrier platforms that have excellent clinical performance.<sup>10,22</sup> Evaluation of the clinical trial data showed that polymeric micellar paclitaxel (Pm-Pac, 230 mg/m<sup>2</sup>) as a first-line therapy can effectively improve the ORR and progression-free survival (PFS) of NSCLC patients with no additional toxic effects occurring after the dosage (standard: 175 mg/m<sup>2</sup>) of paclitaxel increased.<sup>10</sup> However, the disadvantage of clinical trials is that the histopathological information of Pm-Pac-induced toxicity to patients cannot be collected. Understanding the detailed toxicity profile of Pm-Pac in animals will provide potential evidence for future clinical strategy exploration. Therefore, in this study, Sprague–Dawley (SD) rats were used to evaluate the toxic effects induced by Pm-Pac from multiple perspectives, including body weight, peripheral neuropathy symptoms, histopathological profile, and organ, haematological, and biochemical indices.

## Methods

### Preparation of Pm-Pac Nanoparticles

First, 26.5 g of PEG (Mw 2000) (Macklin, China), 25.8 g of DL-lactide (Aladdin, USA), and 1 mL of stannous octoate (0.1 g/mL) (Sigma, USA) were added to an Erlenmeyer flask. Then, 100 mL of dichloromethane (Aladdin, USA) was added as the reaction solvent. The standardized procedure was as follows. Vacuum drying at 80 °C was performed for 6 hours to remove the residual water and dichloromethane. The Erlenmeyer flask was then hermetically sealed under vacuum conditions, and vacuum incubation in an oil bath (Yiheng, China) was carried out at 180 °C for 1 hour. After breaking the Erlenmeyer flask, 50 mL of H<sub>2</sub>O was added and the sample was vortexed at room temperature for 24 hours. Incubation at 70 °C for 1 hour was performed to collect the polymer precipitate before vacuum drying to remove the residual H<sub>2</sub>O. Then, 20 mL of dichloromethane was added, and the mixture was centrifuged at 10,000 r/min for 10 minutes. The supernatant was separated, and 500 mL of anhydrous ether (Shanghai Pharmaceuticals, China) was added to precipitate mPEG 2000-PLA. mPEG 2000-PLA was vacuum dried at room temperature for 24 hours to remove the

residual anhydrous ether and dichloromethane (patent no. CN102181048, Shanghai Yizhong Biotechnical Co., Ltd.). Then, 2.5 g of mPEG 2000-PLA and 0.7 g of paclitaxel (Sigma, USA) were added to an Erlenmeyer flask with 100 mL of acetonitrile as the reaction solvent. Then, the standardized procedure was as follows. Vacuum drying at 50 °C was performed for 2 hours. Next, 50 mL of PBS (pH = 7.0, 20 mM) was added and the solution was filtered through a 0.22 µm membrane before freeze-drying to obtain Pm-Pac (patent no. CN102218027, Shanghai Yizhong Biotechnical Co., Ltd.). High-performance liquid chromatography (HPLC) (Thermo, USA) was used to evaluate the encapsulation rate. The diameter of Pm-Pac was detected with a NICOPM 380ZLS particle size analyser (PSS, USA) (Figure 1).

## Evaluation of Pm-Pac Efficacy in vitro and in vivo

All in vitro and in vivo experiments were approved by the ethics committee of Shanghai Chest Hospital, School of Medicine, Shanghai Jiao Tong University. For cell assays, A549 and H226 cells were obtained from the Shanghai Institute of Biochemistry and Cell Biology. The viability and apoptosis of the NSCLC cell lines were assessed via a CCK8 kit (Dojindo, Japan) and an Annexin V-FITC/PI Apoptosis kit (Zoman Biotechnology, China) according to the manufacturer's protocols. Briefly, for viability determination, 1500 cells per well were cultured in 96-well plates. The cells were exposed to different concentrations (50 µg/mL, 10 µg/mL, 4 µg/mL, 0.4 µg/mL, 0.08 µg/mL, and 0.016 µg/mL) of Pm, Pm-Pac, and Sb-Pac (Chongqing Laimei, China) for 24 hours, and then the absorbance was measured at 450 nm with a spectrophotometric plate reader (Bio-Tek, USA) after incubation with CCK8 reagent. For apoptosis assessments,  $10^5$  cells were cultured in 6-well plates for 12 hours. Then, the cells were exposed to 0.4 µg/mL Pm, Pm-Pac, and Sb-Pac for 24 hours. Cells were stained with propidium iodide (PI) and annexin V-FITC simultaneously and then analysed by flow cytometry (BD LSRFortessa, USA). Establishment of the xenograft tumour model was performed according to our previous study.<sup>23</sup> Briefly, male BALB/c nude mice (aged 4–6 weeks) were purchased from Shanghai Laboratory Animal Center, Shanghai, China. A total of  $10^7$  A549/H226 cells mixed with 100 µL of saline was subcutaneously injected into the right fore-lateral abdomen of each mouse. For the A549-derived animal model, after 3 days of culture, mice with cell-derived xenograft tumours were assigned to 6 groups [Control (Ctrl): saline, 0.2 mL/mouse; Pm: 0.2 mL/mouse; Sb-Pac: 20 mg/kg BW; Pm-Pac (low): 10 mg/kg BW; Pm-Pac (medium): 20 mg/kg BW; Pm-Pac (high): 50.0 mg/kg BW] at equivalent dosages according to body weight. Each mouse received the one treatment every three days (on Day 0, Day 3, Day 6, Day 9, Day 12, Day 15, Day 18, and Day 21), and then the mice were sacrificed on Day 22. For the H226-derived animal model, the processes of group and administration are similar, and then the mice were sacrificed on Day 31. Tumour volume was measured three times per week and was calculated based on the following formula: volume = length × width<sup>2</sup>/2.

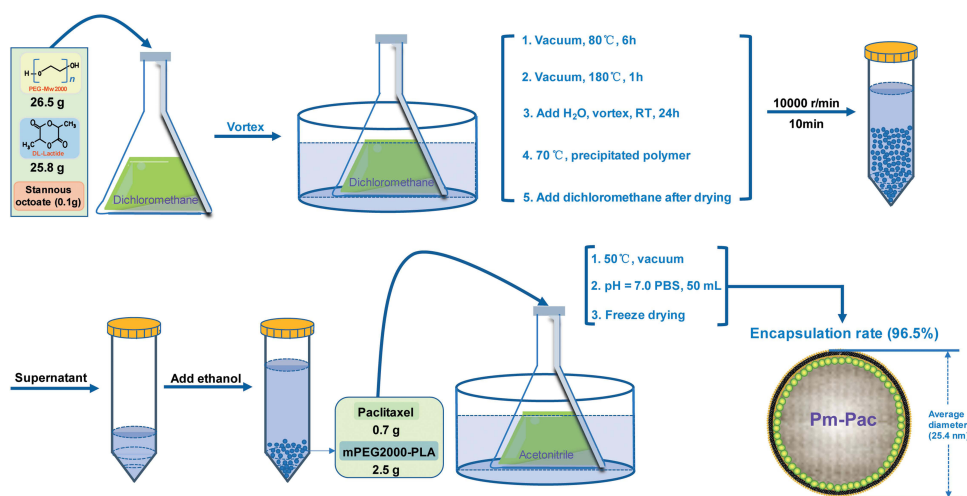


**Figure 1** Generation of polymeric micellar paclitaxel (Pm-Pac) nanoparticles. mPEG 2000-PLA was produced from 2 chemical reactants, PEG-WM 2000 and DL-Lactide, and a series of reactions. Pm-Pac was generated in acetonitrile via the self-assembly of paclitaxel and mPEG 2000-PLA.

## Animals and Treatments

In total, 120 SD rats (including 60 males and 60 females) were purchased from Zhejiang Laboratory Animal Center, Hangzhou, China. Male rats weighing  $200 \pm 10$  g and female rats weighing  $160 \pm 10$  g were left undisturbed to acclimatize for 1 week before the experiments. Sixty rats (30 male and 30 female) were assigned to evaluate short-term toxicity, and the other 60 rats (30 male and 30 female) were assigned to evaluate long-term toxicity. For each toxicity study, sixty rats were assigned to 6 groups [Ctrl: saline, 15.0 mL/kg BW; Pm: 15.0 mL/kg BW; Sb-Pac: 7.0 mg/kg BW; Pm-Pac (low): 14.0 mg/kg BW; Pm-Pac (medium): 23.7 mg/kg BW; Pm-Pac (high): 40.0 mg/kg BW] according to the equivalent factors of sex and body weight. For the assessment of short-term toxicity, each rat received the appropriate treatment once a week for 5 consecutive weeks, and then the mice were sacrificed to determine the organ indices and evaluate organ injury. For the assessment of long-term toxicity, the rats received the same treatments as above for the first 5 weeks and were then allowed to recover for 6 weeks. Finally, the rats were sacrificed to determine the organ indices and evaluate organ injury. All protocols involving animals complied with the national guidelines for the care and use of laboratory animals (Ministry of Health, P.R. China, 1998).

## Dosage Determination of Toxicological Assessment

According to the from BALB/c nude mice results (effective dose = 20 mg/kg BW), the equivalent dose for rats was determined to be 14 mg/kg BW according to a previously introduced method.<sup>24</sup> According to our preexperiment, the body weights of the rats decreased significantly after continuous injection of Pm-Pac (56 mg/kg BW) three times a week. Therefore, we decided on a Pm-Pac dosage of 40 mg/kg BW for the high-dosage experimental group. According to Kadota T et al<sup>25</sup> we used a Sb-Pac dosage of 10 mg/kg BW in the positive control group.

## General Observations

During the experiment, the animal body weights were recorded once a week. Peripheral neuropathy symptoms (including fatigue, general weakness, lying prostrate, tachypnoea and closing eyes) were monitored for 4 hours after drug administration, and then these indicators were checked every day thereafter. Peripheral neuropathy symptoms (including diarrhoea, alopecia, reversal of the hind legs, muscle stiffness, and death) were recorded every day. If the rats experienced peripheral neuropathy symptoms, including fatigue, diarrhoea, alopecia, reversal of the hind legs, muscle stiffness, death, general weakness, lying prostrate, tachypnoea, and closing eyes, the frequency and degree were recorded. The ratios of the symptoms that occurred were calculated at the end of the experiments.

## Organ Weights and Indices

In total, 31 organ samples [including the heart, aorta, spinal cord, lung, kidney, bladder, uterus, ovary, mammary gland, salivary gland, oesophagus, pancreas, adrenal gland, thyroid, parathyroid gland, ischiadic nerve, brain, trachea, stomach, small intestine, large intestine, testis, epididymis, liver, spleen, pituitary gland, prostate, thymus, bone, lymph nodes, and administration site (tail)] were collected after finishing the experimental process. Every organ was weighed, and the organ indices were calculated ((organ weight/body weight)  $\times$  100%).

## Evaluation of Haematological Indices

Rats were fasted 12 hours before blood collection. The red blood cell (RBC), haematocrit (HCT), platelet (PLT), mean platelet volume (MPV), white blood cell (WBC), mean corpuscular volume (MCV), mean corpuscular haemoglobin (MCH), mean corpuscular haemoglobin concentration (MCHC), and red blood cell distribution width (RDW) were determined by laser scattering spectroscopy. Neutrophil (NEUT), lymphocyte (LYMPH), monocyte (MONO), eosinophil (EOS), and basophile (BASO) counts were measured by catalase staining. Reticulocyte (RETIC) evaluations were carried out by RNA staining, haemoglobin (HGB) was assessed by colorimetry, and the prothrombin time (PT) was determined by the agglutination method.



## Evaluation of Blood Biochemical Indices

Rats were fasted 12 hours before blood collection. Aspartate aminotransferase (AST), alanine aminotransferase (ALT), alkaline phosphatase (ALP), and creatine kinase (CK) were examined using International Federation of Clinical Chemistry (IFCC)-guided methods. Blood urea nitrogen (BUN) and triglycerides (TGs) were assessed by a colorimetric method, creatinine (CREA) was evaluated by the Jaffé's method, and total protein (T.P) was determined by the Biuret method. Moreover, albumin (ALB) was investigated by the bromocresol green method, glucose (GLU) was studied by the hexokinase method, total bilirubin (T.BIL) was evaluated by the vanadic acid oxidation method, and total cholesterol (T.CHO) was determined by the Folin method.

## Histopathological Observations

Fresh organs were fixed in 4% PFA for 10 hours and then embedded in molten paraffin. Tissue sections approximately 5  $\mu$ m thick were deparaffinized and then stained with haematoxylin and eosin (HE) for histological examinations. Histological observations of various organ sections were made under a light microscope at a magnification of 100 $\times$  (Olympus, Japan). Evaluation of the histopathological images was performed with a pathological image analysis system (Pixar, USA).

## Statistical Analysis

The data are presented as the mean  $\pm$  standard deviation. Differences between groups were analysed using one-way analysis of variance (ANOVA) and Duncan's multiple range tests. A *P* value < 0.05 indicated a significant difference between groups.

## Results

### Preparation and Antitumour Efficacy of Pm-Pac

The preparation of the nanoparticle Pm-Pac is illustrated in [Figure 1](#). First, mPEG 2000-PLA was synthesized by the designed reaction between PEG-Mw 2000 and DL-lactide. Second, the self-assembly of mPEG 2000-PLA and paclitaxel was performed to obtain Pm-Pac with a size of  $\approx$ 25.4 nm and encapsulation efficiency of  $\approx$ 96.5%. Cell viability analysis suggested that Pm-Pac can induce slightly more inhibitory efficacy than Sb-Pac in the NSCLC cell lines A549 and H226 in vitro ([Figure 2A](#) and [B](#)). Cell apoptosis analysis suggested that Pm-Pac can induce more A549 and H226 cell apoptosis than Sb-Pac in vitro ([Figure 2C](#) and [D](#)). Furthermore, we performed an in vivo experiment to evaluate the antitumour efficacy of Pm-Pac. Compared with Sb-Pac, Pm-Pac showed markedly enhanced tumour growth inhibition efficacy in an A549-derived xenograft tumour model ([Figure 2E](#) and [F](#)). These results suggested that the nanoparticle Pm-Pac has potential application value for improving the therapeutic efficacy of paclitaxel, but the toxicity profile of Pm-Pac is still unclear.

### Effects of Pm-Pac on Body Weight, Peripheral Neuropathy and Organ Indices from the Short-Term Toxicological Observations

In this study, we evaluated the toxic effects of Pm-Pac on healthy SD rats. After the administration of Pm-Pac and Sb-Pac once a week for 5 consecutive weeks, we found that the body weights of the rats in the treatment groups decreased significantly compared to those in the Ctrl and Pm groups. Among the treatment groups, the body weights of the rats who were administered Pm-Pac (40 mg/kg) decreased more remarkably, suggesting that potential intolerable toxicity occurred at this dosage ([Figure 3A](#), [Supplementary Table 1](#)).

The incidence of peripheral neuropathy chemotherapy-related side effects ranges from 11% to 87%, with the highest value reported for paclitaxel.<sup>26</sup> Here, we observed peripheral neuropathy symptoms in healthy SD rats after Sb-Pac administration and Pm-Pac administration ([Table 1](#)). In the Ctrl and Pm groups, none of the rats experienced peripheral neuropathy symptoms throughout the experiment. In the Sb-Pac group, all rats displayed peripheral neuropathy symptoms, including fatigue, general weakness, lying prostrate, tachypnoea, and closing eyes. These symptoms basically disappeared within 3 hours after the first administration and within 1 hour after the fifth administration, suggesting the

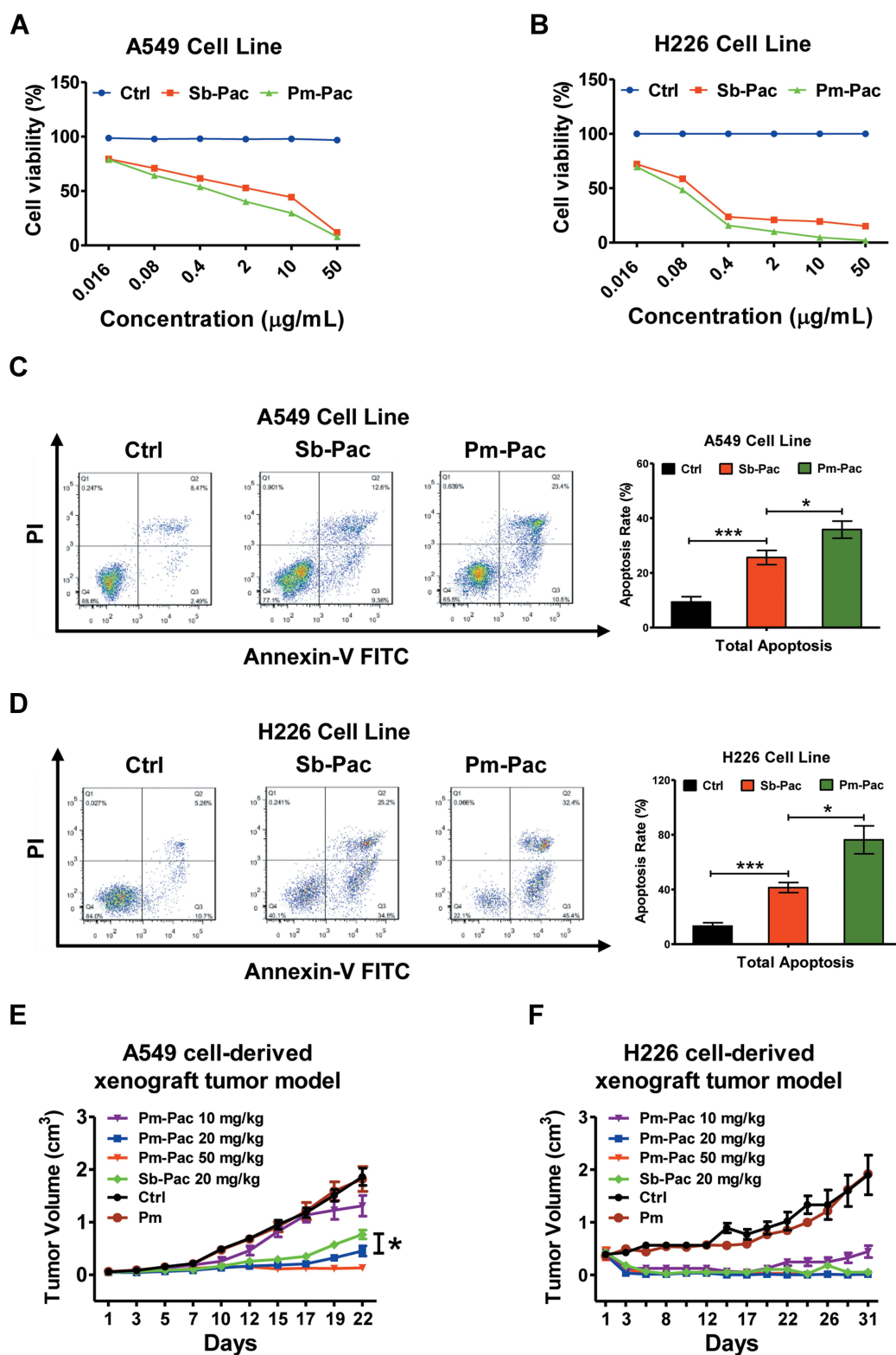


**Figure 2** Pm-Pac-induced antitumour activity in vitro and in vivo. **(A)** The antitumour activity of Pm-Pac-induced cell viability inhibition was assessed in A549 cells in vitro ( $n = 3$ ). **(B)** The antitumour activity of Pm-Pac-induced cell viability inhibition was assessed in H226 cells in vitro ( $n = 3$ ). **(C)** The antitumour activity of Pm-Pac-induced cell apoptosis was assessed in A549 cells in vitro ( $n = 3$ ,  $*P < 0.05$ ,  $***P < 0.001$ ). **(D)** The antitumour activity of Pm-Pac-induced cell apoptosis was assessed in H226 cells in vitro ( $n = 3$ ,  $*P < 0.05$ ,  $***P < 0.001$ ). **(E and F)** The antitumour activity of Pm-Pac was assessed in A549/H226 cell-derived xenograft tumour model ( $n = 8$ ,  $*P < 0.05$ ).

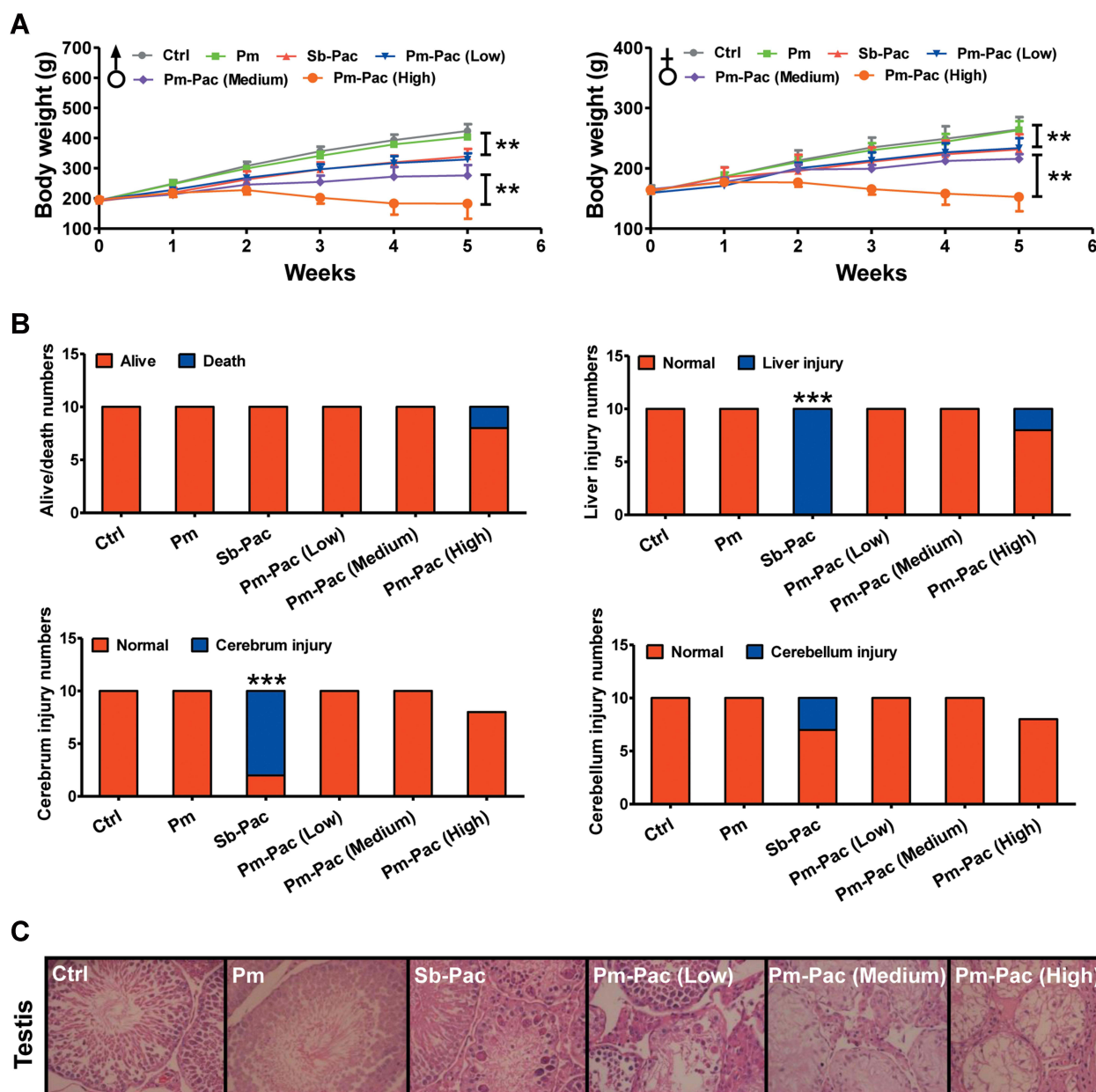


**Figure 3** Pm-Pac-induced short-term toxicity to healthy SD rats. Sixty SD rats were allocated to 6 groups [Ctrl, Pm, Sb-Pac (7 mg/kg), and Pm-Pac (low: 14 mg/kg, medium: 23.7 mg/kg, and high: 40 mg/kg)] and received the corresponding treatment once a week for 5 consecutive weeks. **(A)** Effects of the polymeric micellar paclitaxel (Pm-Pac) nanoparticle on the body weights of healthy SD rats. Left: body weights of male rats ( $n = 5$ ,  $**P < 0.01$ ); right: body weights of female rats ( $n = 5$ ,  $**P < 0.01$ ). **(B)** Evaluation of Pm-Pac-induced death, liver injury, cerebral injury, and cerebellar injury after administration once a week for 5 consecutive weeks ( $n = 10$ ,  $***P < 0.001$ ). **(C)** Pathological evaluation of Pm-Pac-induced testicular toxicity to healthy SD rats ( $n = 5$ , HE, 100 $\times$ ).

emergence of some adaptation with the number of administrations. Furthermore, 30% of the rats experienced diarrhoea, 50% experienced alopecia, 10% experienced reversal of hind legs, and 60% experienced muscle stiffness. In the Pm-Pac (low, medium, and high) groups, the peripheral neuropathy symptoms, including general weakness, lying prostrate, tachypnoea, and closing eyes, were similar to those in the Sb-Pac group. The longer the dosage of Pm-Pac was administered, the longer the duration of peripheral neuropathy symptoms. However, there were differences in the other peripheral neuropathy symptoms in rats with different administered dosages of Pm-Pac. In the Pm-Pac (low) group, 100% of the female rats experienced alopecia, and 20% experienced muscle stiffness. In the Pm-Pac (medium) group, 30% of the rats experienced fatigue, 10% experienced diarrhoea, 100% experienced alopecia, and 50% experienced muscle stiffness. Alopecia recovered in these rats until 3 weeks after the last administration. In the Pm-Pac (high)

**Table 1** Observation of Pm-Pac-Induced Peripheral Neuropathy Symptoms After the Sb-Pac and Sb-Pac Administration

Groups (n = 10)		Fatigue	Diarrhea	Alopecia	Reverse the Hind Legs	Muscle Stiffness	General Weakness	Lie Prostrate	Tachypnea	Closing Eyes
<b>Ctrl</b>	Total (%)	0	0	0	0	0	0	0	0	0
	Male (%)	0	0	0	0	0	0	0	0	0
	Female (%)	0	0	0	0	0	0	0	0	0
<b>Pm</b>	Total (%)	0	0	0	0	0	0	0	0	0
	Male (%)	0	0	0	0	0	0	0	0	0
	Female (%)	0	0	0	0	0	0	0	0	0
<b>Sb-Pac</b>	Total (%)	100%	30%	50%	10%	60%	100%	100%	100%	100%
	Male (%)	100%	40%	20%	0	40%	100%	100%	100%	100%
	Female (%)	100%	20%	80%	20%	80%	100%	100%	100%	100%
<b>Pm-Pac (Low)</b>	Total (%)	0	0	50%	0	10%	100%	100%	100%	100%
	Male (%)	0	0	0	0	0	100%	100%	100%	100%
	Female (%)	0	0	100%	0	20%	100%	100%	100%	100%
<b>Pm-Pac (Medium)</b>	Total (%)	30%	10%	100%	0	50%	100%	100%	100%	100%
	Male (%)	20%	20%	100%	0	40%	100%	100%	100%	100%
	Female (%)	40%	0	100%	0	60%	100%	100%	100%	100%
<b>Pm-Pac (High)</b>	Total (%)	100%	40%	100%	100%	100%	100%	100%	100%	100%
	Male (%)	100%	60%	100%	100%	100%	100%	100%	100%	100%
	Female (%)	100%	20%	100%	100%	100%	100%	100%	100%	100%

group, 100% of the rats experienced fatigue, 40% experienced diarrhoea (one rat died after each the fourth administration and fifth administration), 100% experienced alopecia (within 3 days after the first administration), 100% experienced reversal of the hind legs, and 100% experienced muscle stiffness. Alopecia recovered in these rats until 4 weeks after the last administration, diarrhoea recovered until 2 weeks after the last administration, and the other symptoms, including reversal of the hind legs and muscle stiffness, recovered until 3 weeks after the last administration. These results suggested that Pm-Pac can reduce the incidence of peripheral neuropathy.

Furthermore, by analysing the changes in organ weights and indices, we found that the weights/indices of the testis and epididymis in the Pm-Pac groups decreased significantly compared with those in the Sb-Pac group, suggesting that Pm-Pac is potentially more toxic to these targeted organs than Sb-Pac ([Supplementary Table 1](#)).

## Effects of Pm-Pac on Haematological and Biochemical Indices from the Short-Term Toxicological Observations

Among the haematological indices, we found that WBCs and LYMPHs decreased significantly, and the RDW and RETICs increased remarkably after both Sb-Pac administration and Pm-Pac administration. More severe toxicity was observed from the blood indices (enhanced RBCs, HCT and MCH; decreased MONOs) in the Pm-Pac (high) group. Haematological index abnormalities occurred in only the Pm-Pac groups, including decreased NEUTs, decreased MONOs, and decreased EOSs ([Supplementary Table 2](#)). Regarding the blood biochemical indices, our results indicated that Sb-Pac did not show significant alterations, except for decreased GLU; Pm-Pac-induced biochemical index alterations included increased ALT, decreased ALB, decreased T.P, and decreased CREA. Consistent with the above results, more severe toxicity was observed from the biochemical index abnormalities (such as ALT, AST, GLU, ALB, CREA, TG, Na<sup>+</sup>, and Cl<sup>-</sup>) in the Pm-Pac (high) group ([Supplementary Table 3](#)). These results suggested that high-dosage Pm-Pac-induced toxicity is intolerable, while the toxicity caused by the low and medium dosages of Pm-Pac is potentially acceptable.

## Histopathological Alterations Caused by Pm-Pac from the Short-Term Toxicological Observations

Pathological examination was performed to observe changes in the microstructures of all 31 organs. After administration of Pm-Pac (40 mg/kg) for 5 consecutive weeks, we found that the microstructures of the organs, including the heart, aorta, spinal cord, lung, kidney, bladder, uterus, ovary, mammary gland, salivary gland, oesophagus, pancreas, adrenal gland, thyroid, parathyroid gland, ischiadic nerve, hypophysis, trachea, stomach, small intestine, and large intestine, were normal ([Supplementary Figure 1](#)). However, for those rats who received different dosages of Pm-Pac and Sb-Pac, we found that the organs, including the thymus, testis, epididymis, bone marrow, lymph node, spleen, and prostate, showed atrophy or injury ([Supplementary Figure 2](#)). In particular, the rats treated with Sb-Pac (7 mg/kg) and Pm-Pac (40 mg/kg) had more toxic reactions ([Figure 3B](#), [Supplementary Figure 2](#)). Among the 10 rats in the Sb-Pac group, 8 showed cerebral injury (multiple instances of malacia in the cortex, nuclear debris, increased macrophages, and gliocyte hyperplasia along with vacuolar degeneration of nerve fibres), 3 showed cerebellar injury (degeneration and necrosis of neurocytes in the stratum granulosum, necrosis, nuclear pyknosis and histocyte infiltration), and all 10 rats showed liver injury (mild extramedullary haematopoiesis) ([Figure 3B](#), [Supplementary Figure 2](#)). Among the 10 rats in the Pm-Pac (40 mg/kg) group, the 2 male rats that died showed multiple organ failure (data not shown), and the other 3 male rats showed more severe testicular atrophy (atrophy of the convoluted seminiferous tubules, thickening of the outer membrane, interstitial oedema, diffuse interstitial cell proliferation) ([Figure 3C](#)). These results demonstrated that the paclitaxel-induced short-term toxic reaction in rats could be decreased with the Pm-Pac formulation. However, Pm-Pac-induced long-term toxicity is still elusive.

## Long-Term Toxicity of Pm-Pac to Healthy Rats

To determine the long-term toxicity of Pm-Pac, macroscopic and pathological examinations were performed on the rats that had recovered for 6 weeks after the last administrations of Pm-Pac and Sb-Pac ([Figures 4 and 5](#)). The body weights of the Pm-Pac (40 mg/kg)-treated rats decreased significantly, indicating intolerable toxicity induced by Pm-Pac at this dosage ([Figure 4A](#)). According to the results from the macroscopic examination, all of the organs from the Pm-Pac (14 mg/kg)-treated and Pm-Pac (23.7 mg/kg)-treated rats showed no visual abnormalities (data not shown). However, the weights and indices of the organs, including the thymus gland, testis, and epididymis, were significantly decreased after further examination ([Supplementary Table 1](#)). However, in the Pm-Pac (high) group, the organs, including the testis and epididymis, showed both visual abnormalities and weight/index abnormalities ([Supplementary Table 1](#)). After recovery for 6 weeks, the pathological examination suggested that the majority of the organs were normal and that the main liver and brain toxicity of Sb-Pac had decreased significantly, but genital system toxicity was still observed in all rats treated with Sb-Pac/Pm-Pac ([Figure 4B and C](#), [Supplementary Figures 3 and 4](#)). The results indicated irreversible atrophy of the testis and epididymis in all paclitaxel-treated rats (including Sb-Pac and Pm-Pac) ([Figure 4C and 5](#)). The Pm-Pac-induced long-term toxicity as evaluated by the haematological indices was also acceptable after 6 weeks of recovery, except in the Pm-Pac (high) group ([Supplementary Tables 2 and 3](#)). These results suggested that doubling the paclitaxel dosage using a nanoparticle Pm delivery system did not increase paclitaxel-induced toxicity to healthy rats.

## Discussion

Chemotherapy has always played an indispensable role in the historical treatment of NSCLC.<sup>9,10,27</sup> Although new therapeutic regimens (such as immunotherapy and targeted therapy) have attempted to bring NSCLC clinical treatment into a chemo-free stage,<sup>28–31</sup> recent clinical trials have demonstrated that the ORR and OS can be greatly improved when these regimens are combined with chemotherapy,<sup>11,12,32</sup> suggesting that chemotherapy is indispensable, at least at present. However, how to reduce chemotherapy-induced systemic toxicity has always been a hot issue in the field of cancer therapy. Previous studies have discussed the pharmacokinetic profiles and clinical efficacy of Pm-Pac in clinical trials.<sup>10,19,22</sup> In this study, we found that Pm-Pac (2~3-fold greater dosage than Sb-Pac) can significantly reduce the incidences of peripheral neuropathy, brain injury and liver injury in terms of both short-term and long-term toxicity to healthy SD rats and induce potential male genital system toxicity (testicular atrophy and prostatic atrophy).

Paclitaxel is one of the most conventional chemotherapeutic drugs for NSCLC in clinical practice. The molecular mechanism of the paclitaxel-induced anticancer effect includes ① direct effects on the tubulin dimers of microtubules to



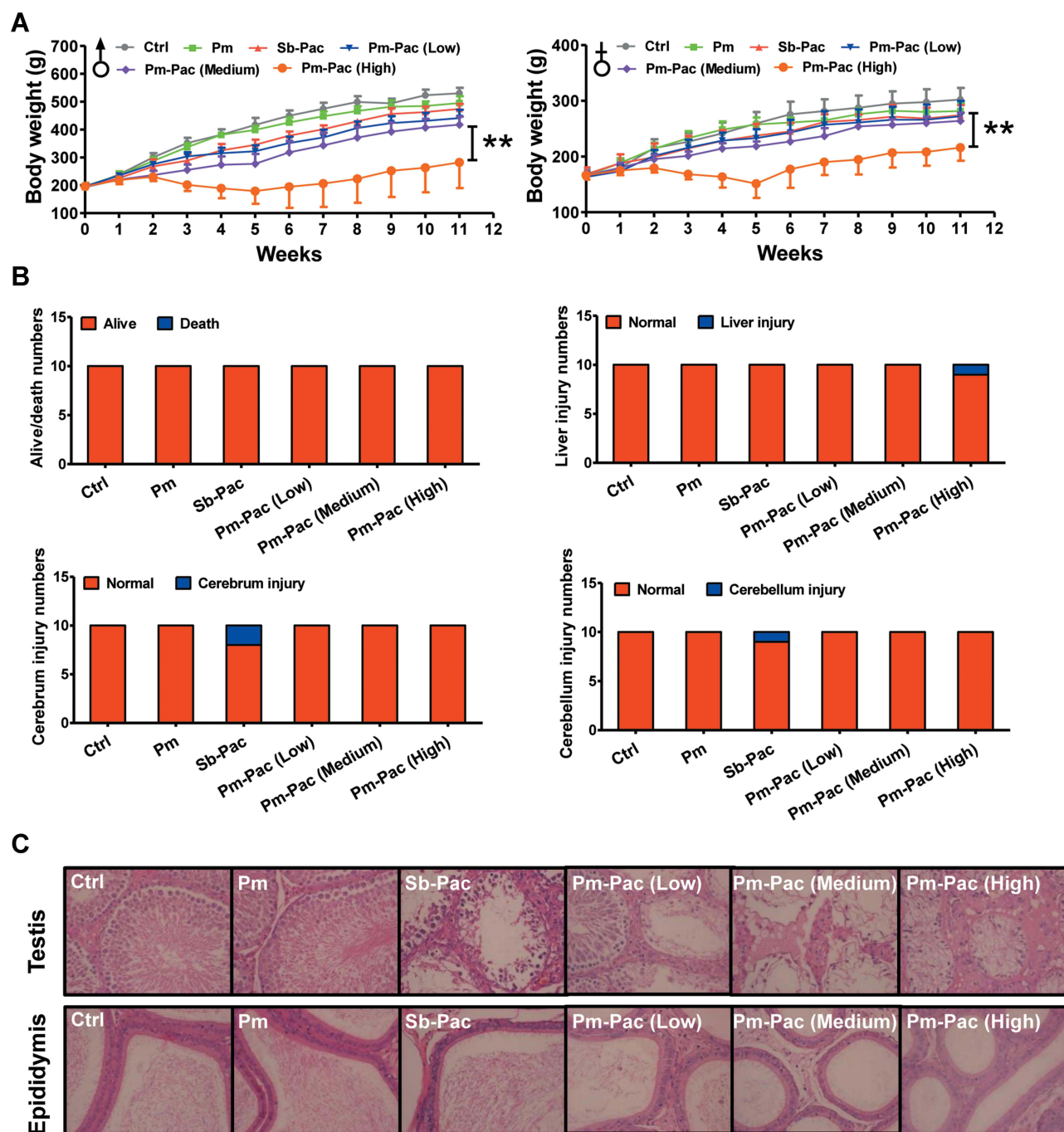
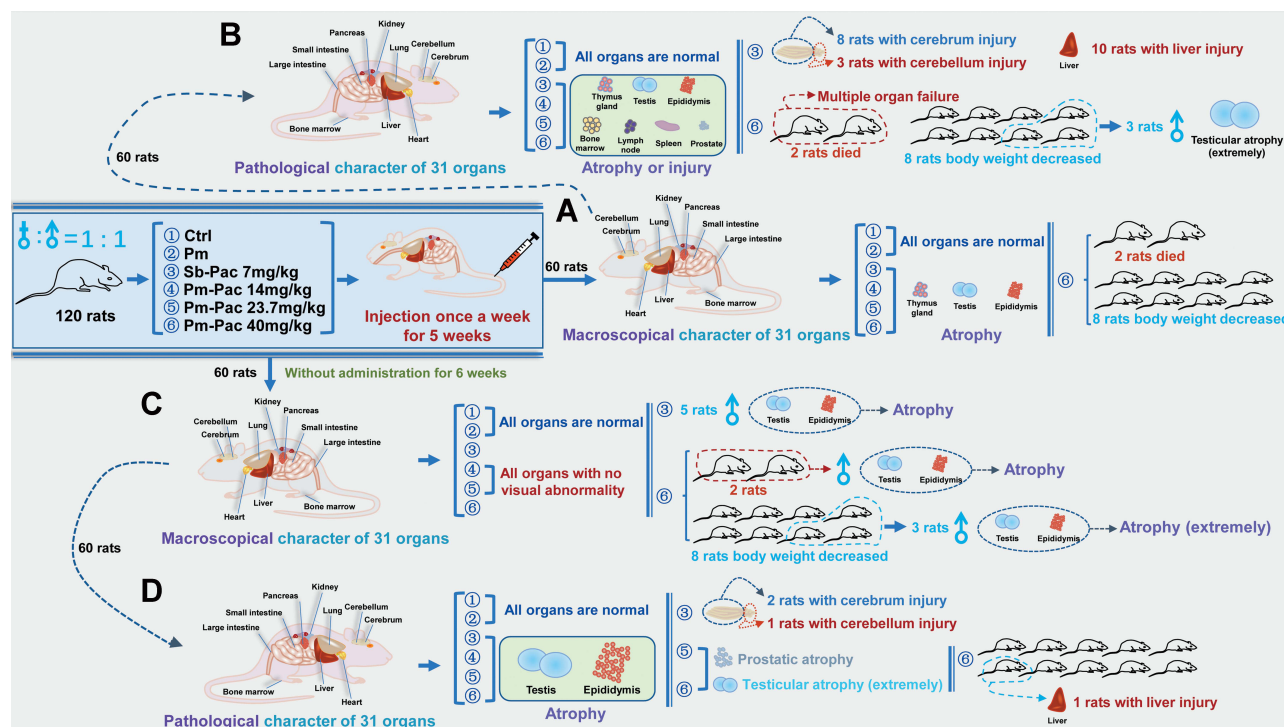


**Figure 4** Pm-Pac-induced long-term toxicity to healthy SD rats. Sixty SD rats were allocated to 6 groups [Ctrl, Pm, Sb-Pac (7 mg/kg), and Pm-Pac (low: 14 mg/kg, medium: 23.7 mg/kg, and high: 40 mg/kg)] and received the corresponding treatment once a week for 5 consecutive weeks and were then allowed to recover for 6 weeks. **(A)** Effects of the polymeric micellar paclitaxel (Pm-Pac) nanoparticle on the body weights of healthy SD rats. Left: body weights of male rats ( $n = 5$ ); right: body weights of female rats ( $n = 5$ ,  $**P < 0.01$ ). **(B)** Evaluation of Pm-Pac-induced death, liver injury, cerebral injury, and cerebellar injury after administration once a week for 5 consecutive weeks and then recovery for 6 weeks ( $n = 10$ ). **(C)** Pathological evaluation of Pm-Pac-induced testicular and epididymal toxicity to healthy SD rats ( $n = 5$ , HE, 100 $\times$ ).

cause them to lose their dynamic balance<sup>33</sup> and ② promotion of tubulin polymerization and microtubule assembly and prevention of depolymerization to allow microtubule stability, inhibit cancer cell mitosis and induce apoptosis, thus effectively preventing the proliferation of cancer cells.<sup>34</sup> Nevertheless, tubulin, an important component taking part in cell mitosis, is ubiquitous in eukaryotic cells. Conventional solvent-based paclitaxel can be widely distributed in the body and then induce damage to the peripheral nervous system, normal organs and tissues, resulting in treatment-related



dosing difficulties (recommended dosage:  $175 \text{ mg/m}^2$ ).<sup>10</sup> Nanodelivery platforms can potentially decrease drug-related toxicity, although some nanoparticles are distributed in the liver and spleen. However, the merits of nanoparticles have also been shown to be significant, as they can accumulate in tumour cells or tissues for a long time.<sup>16</sup> Pm is a nanocarrier delivery platform developed by Shanghai Yizhong Biotechnical Co., Ltd. that can significantly reduce paclitaxel-induced toxicity. A Phase I clinical trial provided a safe dose range of  $175\text{--}435 \text{ mg/m}^2$  for cancer patients.<sup>19</sup> Our randomized phase III clinical trial suggests a dose range of  $230 \text{ mg/m}^2$  to  $300 \text{ mg/m}^2$ , which provides a safe dosage and better ORR and PFS without grade 2–4 haematological toxicity.<sup>10</sup> These clinical results suggest that Pm-Pac can reduce paclitaxel-induced toxicity and improve chemotherapeutic efficacy in NSCLC patients.

The incidence of peripheral neuropathy prevents an increase in the administered dose of paclitaxel to enhance the antitumour effect.<sup>26</sup> Previous studies have demonstrated that paclitaxel-induced neuropathy usually presents as numbness, dysesthesias, altered proprioception, paraesthesia, and a loss of dexterity in the toes and fingers.<sup>35</sup> Further analysis suggested that paclitaxel-induced microtubule disruption and ion channel alterations can explain most peripheral neuropathy symptoms.<sup>26</sup> In brief, the mechanisms of peripheral neuropathy include microtubule disruption,<sup>36</sup> mitochondrial dysfunction,<sup>37</sup> axon degeneration,<sup>36</sup> altered calcium homeostasis,<sup>38</sup> changes in peripheral nerve excitability,<sup>39</sup> immune processes and neuroinflammation.<sup>40</sup> Here, our results suggested that paclitaxel induced peripheral neuropathy symptoms in healthy rats, including fatigue, diarrhoea, alopecia, reversal of hind legs, muscle stiffness, general weakness, lying prostrate, tachypnoea, and closing eyes. Interestingly, our results also demonstrated that Pm-Pac (low, 2-fold the dosage of Sb-Pac) can reduce the incidence of peripheral neuropathy in healthy rats.

Understanding the pathological profiling of Pm-Pac-induced toxicity is a very important issue for clinical practice that potentially affects the indications for combined treatment. First, SD rats were administered Pm-Pac at different dosages for 5 consecutive weeks (short-term toxicity) and were then allowed to recover for 6 weeks (long-term toxicity). A total of 31 organs were collected from each rat, and then the organ weights and indices were determined. Second, the haematological and

biochemical indices were investigated for each rat, and then the Pm-Pac-induced toxicity on the haematological and metabolic organs was evaluated. Finally, we performed HE staining to examine all 31 collected organs and then evaluated Pm-Pac-induced toxicity in these organs. Paclitaxel-induced toxicity (including sensory neuropathy, gastrointestinal reaction, liver injury, and so on) usually occurs in clinical practice.<sup>10</sup> In this study, we found that the majority of rat organs (including the heart, aorta, spinal cord, lung, kidney, bladder, uterus, ovary, mammary gland, salivary gland, oesophagus, pancreas, adrenal gland, thyroid, parathyroid gland, ischiadic nerve, hypophysis, trachea, stomach, small intestine, and large intestine) were not injured when the dosage of Pm-Pac reached 40 mg/kg body weight or when the dosage of Sb-Pac reached 7 mg/kg body weight. Interestingly, we found that Pm-Pac can decrease liver injury, cerebral injury, cerebellar injury, and drug administration-induced mortality compared with Sb-Pac. Furthermore, male genital system toxicity rather than female genital system toxicity induced by Pm-Pac is worth considering. After the abovementioned examinations, we found that the Pm-Pac-induced short-term toxicity to healthy rats did not significantly increase, even when the dose was 3-fold greater than that of Sb-Pac. During the long-term observations, the toxicity of the 2-fold dosage of Pm-Pac was still lower than that induced by Sb-Pac. Collectively, these results provide potential evidence for future clinical strategy exploration (especially combination strategies of Pm-Pac plus immunotherapy, antiangiogenic therapy, or TKI therapy).

## Conclusion

In summary, we systematically evaluated the ability of Pm-Pac engineered nanoparticles to reduce toxicity to SD rats. In the present study, we provide the first histopathological examination of the Pm-Pac-induced toxicity profile in healthy rats. Therefore, this work provides a novel perspective on the development of nanomedicines to investigate chemotherapeutic toxicity to SD rats and a potential basis for the exploration of future clinical combination strategies.

## Abbreviations

NSCLC, Non-small cell lung cancer; Pm-Pac, Polymeric micellar paclitaxel; Pm, Polymeric micellar; Sb-Pac, solvent-based paclitaxel; SD, Sprague-Dawley; OS, Overall survival; TKI, Tyrosine kinase inhibitor; ORR, Objective response rate; PFS, Progression-free survival; HPLC, High-performance liquid chromatography; PI, Propidium iodide; Ctrl, Control; BW, Body weight; RBC, Red blood cell; HCT, Hematocrit; PLT, Platelet; MPV, Mean platelet volume; WBC, White blood cell; MCV, Mean corpuscular volume; MCH, Mean corpuscular hemoglobin; MCHC, Mean corpuscular hemoglobin concentration; RDW, Red blood cell distribution width; NEUT, Neutrophil; LYMPH, Lymphocyte; MONO, Monocyte; EOS, Eosinophils; BASO, Basophile; RETIC, Reticulocyte; HGB, Hemoglobin; PT, Prothrombin time; ALT, Alanine aminotransferase; AST, Aspartate aminotransferase; ALP, Alkaline phosphatase; CK, Creatine kinase; IFCC, International Federation of Clinical Chemistry; BUN, Blood urea nitrogen; TG, Triglyceride; CREA, Creatinine; T.P, Total protein; ALB, Albumin; GLU, Glucose; T.BIL, Total bilirubin; T.CHO, Total cholesterol; HE, Hematoxylin and eosin.

## Data Sharing Statement

The data that support the findings of this study are available from the corresponding author upon reasonable request. Some data may not be made available because of privacy or ethical restrictions.

## Ethics Statement

All experimental protocols were and approved by the Ethics Committee Shanghai Chest Hospital, School of Medicine, Shanghai Jiao Tong University and Shanghai Yizhong Biotechnical Co., Ltd.

## Funding

This work was supported by the foundation of National Natural Science Foundation of China grants (Project No. 82272913); Shanghai Chest Hospital (Project No. 2019YNJCM11 & YJXT20190102); the Shanghai Leading Talents Program (2013), the program of Shanghai Jiao Tong University (Project No. YG2021QN121); the foundation of Chinese society of clinical oncology (Project No. Y-2019AZD-0355 & Y-QL2019-0125); National Multi-disciplinary Treatment Project for Major Disease (Project No. 2020NMDTP).

## Disclosure

The authors report no conflicts of interest in this work.

## References

- Lu J, Zhang Y, Lou Y, et al. ctDNA-Profilng-Based UBL biological process mutation status as a predictor of atezolizumab response among TP53-negative NSCLC patients. *Front Genet.* 2021;12:723670. doi:10.3389/fgene.2021.723670
- Lu J, Zhong H, Wu J, et al. Circulating DNA-based sequencing guided anlotinib therapy in non-small cell lung cancer. *Adv Sci.* 2019;6(19):1900721. doi:10.1002/advs.201900721
- Lu J, Zhong R, Lou Y, et al. TP53 mutation status and biopsy lesion type determine the immunotherapeutic stratification in non-small-cell lung cancer. *Front Immunol.* 2021;12:732125. doi:10.3389/fimmu.2021.732125
- Gridelli C, Rossi A, Carbone DP, et al. Non-small-cell lung cancer. *Nat Rev Dis Primers.* 2015;1(1):15009. doi:10.1038/nrdp.2015.9
- Lu J, Zhang W, Yu K, et al. Screening anlotinib responders via blood-based proteomics in non-small cell lung cancer. *FASEB J.* 2022;36:e22465. doi:10.1096/fj.202101658R
- Lu J, Wu J, Lou Y, et al. Blood-based tumour mutation index act as prognostic predictor for immunotherapy and chemotherapy in non-small cell lung cancer patients. *Biomark Res.* 2022;10(1):55. doi:10.1186/s40364-022-00400-5
- Herbst RS, Morgensztern D, Boshoff C. The biology and management of non-small cell lung cancer. *Nature.* 2018;553(7689):446–454. doi:10.1038/nature25183
- Luo Q, Duan Z, Li X, et al. Branched polymer-based redox/enzyme-activatable photodynamic nanoagent to trigger STING-Dependent immune responses for enhanced therapeutic effect. *Adv Funct Mater.* 2022;32(13):2110408. doi:10.1002/adfm.202110408
- Chu T, Lu J, Bi M, et al. Equivalent efficacy study of QL1101 and bevacizumab on untreated advanced non-squamous non-small cell lung cancer patients: a Phase 3 randomized, double-blind clinical trial. *Cancer Biol Med.* 2021;18(3):816–824. doi:10.20892/j.issn.2095-3941.2020.0212
- Shi M, Gu A, Tu H, et al. Comparing nanoparticle polymeric micellar paclitaxel and solvent-based paclitaxel as first-line treatment of advanced non-small-cell lung cancer: an open-label, randomized, multicenter, phase III trial. *Ann Oncol.* 2021;32(1):85–96. doi:10.1016/j.annonc.2020.10.479
- Han B, Jin B, Chu T, et al. Combination of chemotherapy and gefitinib as first-line treatment for patients with advanced lung adenocarcinoma and sensitive EGFR mutations: a randomized controlled trial. *Int J Cancer.* 2017;141(6):1249–1256. doi:10.1002/ijc.30806
- Gandhi L, Rodríguez-Abreu D, Gadgeel S, et al. Pembrolizumab plus chemotherapy in metastatic non-small-cell lung cancer. *N Engl J Med.* 2018;378(22):2078–2092. doi:10.1056/NEJMoa1801005
- Lu J, Chu T, Liu H, et al. Equivalent efficacy assessment of QL1101 and bevacizumab in nonsquamous non-small cell lung cancer patients: a two-year follow-up data update. *Chin J Cancer Res.* 2022;34(1):1–12. doi:10.21147/j.issn.1000-9604.2022.01.03
- Wei G, Wang Y, Yang G, Wang Y, Ju R. Recent progress in nanomedicine for enhanced cancer chemotherapy. *Theranostics.* 2021;11(13):6370–6392. doi:10.7150/thno.57828
- Norouzi M, Hardy P. Clinical applications of nanomedicines in lung cancer treatment. *Acta Biomater.* 2021;121:134–142. doi:10.1016/j.actbio.2020.12.009
- Luo L, Qi Y, Zhong H, et al. GSH-sensitive polymeric prodrug: synthesis and loading with photosensitizers as nanoscale chemo-photodynamic anti-cancer nanomedicine. *Acta Pharm Sin B.* 2022;12(1):424–436. doi:10.1016/j.apsb.2021.05.003
- Tan P, Cai H, Wei Q, et al. Enhanced chemo-photodynamic therapy of an enzyme-responsive prodrug in bladder cancer patient-derived xenograft models. *Biomaterials.* 2021;277:121061. doi:10.1016/j.biomaterials.2021.121061
- Mangal S, Gao W, Li T, Zhou QT. Pulmonary delivery of nanoparticle chemotherapy for the treatment of lung cancers: challenges and opportunities. *Acta Pharmacol Sin.* 2017;38:782–797. doi:10.1038/aps.2017.34
- Shi M, Sun J, Zhou J, et al. Phase I dose escalation and pharmacokinetic study on the nanoparticle formulation of polymeric micellar paclitaxel for injection in patients with advanced solid malignancies. *Invest New Drugs.* 2018;36(2):269–277. doi:10.1007/s10637-017-0506-4
- Rugo HS, Barry WT, Moreno-Aspitia A, et al. Randomized phase III trial of paclitaxel once per week compared with nanoparticle albumin-bound nab-paclitaxel once per week or ixabepilone with bevacizumab as first-line chemotherapy for locally recurrent or metastatic breast cancer: CALGB 40502/NCCTG N063H (Alliance). *J Clin Oncol.* 2015;33(21):2361–2369. doi:10.1200/JCO.2014.59.5298
- Shi J, Kantoff PW, Wooster R, Farokhzad OC. Cancer nanomedicine: progress, challenges and opportunities. *Nat Rev Cancer.* 2017;17:20–37. doi:10.1038/nrc.2016.108
- Lu J, Gu A, Wang W, et al. Polymeric micellar paclitaxel (Pm-Pac) prolonged overall survival for NSCLC patients without pleural metastasis. *Int J Pharm.* 2022;623:121961. doi:10.1016/j.ijpharm.2022.121961
- Lu J, Zhong H, Chu T, et al. Role of anlotinib-induced CCL2 decrease in anti-angiogenesis and response prediction for nonsmall cell lung cancer therapy. *Eur Respir J.* 2019;53(3):1801562. doi:10.1183/13993003.01562-2018
- Nair AB, Jacob S. A simple practice guide for dose conversion between animals and human. *J Basic Clin Pharm.* 2016;7(2):27–31. doi:10.4103/0976-0105.177703
- Kadota T, Chikazawa H, Kondoh H, et al. Toxicity studies of paclitaxel. (II)--One-month intermittent intravenous toxicity in rats. *J Toxicol Sci.* 1994;19(Suppl 2):11–34. doi:10.2131/jts.19.Supplement1\_11
- Zajackowska R, Kocot-Kępska M, Leppert W, et al. Mechanisms of chemotherapy-induced peripheral neuropathy. *Int J Mol Sci.* 2019;20(6):1451. doi:10.3390/ijms20061451
- Ettinger DS, Wood DE, Aisner DL, et al. NCCN guidelines insights: non-small cell lung cancer, version 2.2021. *J Natl Compr Canc Netw.* 2021;19(3):254–266. doi:10.6004/jnccn.2021.0013
- Mok TS, Wu Y-L, Thongprasert S, et al. Gefitinib or Carboplatin–paclitaxel in pulmonary adenocarcinoma. *N Engl J Med.* 2009;361(10):947–957. doi:10.1056/NEJMoa0810699
- Reck M, Rodríguez-Abreu D, Robinson AG, et al. Pembrolizumab versus Chemotherapy for PD-L1-positive non-small-cell lung cancer. *N Engl J Med.* 2016;375(19):1823–1833. doi:10.1056/NEJMoa1606774



30. Rittmeyer A, Barlesi F, Waterkamp D, et al. Atezolizumab versus docetaxel in patients with previously treated non-small-cell lung cancer (OAK): a phase 3, open-label, multicentre randomised controlled trial. *Lancet*. 2017;389(10066):255–265. doi:10.1016/S0140-6736(16)32517-X
31. Mok TS, Wu Y-L, Ahn M-J, et al. Osimertinib or Platinum–Pemetrexed in EGFR T790M–positive lung cancer. *N Engl J Med*. 2017;376(7):629–640. doi:10.1056/NEJMoa1612674
32. Nishio M, Barlesi F, West H, et al. Atezolizumab plus chemotherapy for first-line treatment of nonsquamous NSCLC: results from the randomized phase 3 IMpower132 trial. *J Thorac Oncol*. 2021;16(4):653–664. doi:10.1016/j.jtho.2020.11.025
33. Jordan MA, Wilson L. Microtubules as a target for anticancer drugs. *Nat Rev Cancer*. 2004;4(4):253–265. doi:10.1038/nrc1317
34. Weaver BA, Bement W. How Taxol/paclitaxel kills cancer cells. *Mol Biol Cell*. 2014;25(18):2677–2681. doi:10.1091/mbc.e14-04-0916
35. De Iuliis F, Taglieri L, Salerno G, Lanza R, Scarpa S. Taxane induced neuropathy in patients affected by breast cancer: literature review. *Crit Rev Oncol Hematol*. 2015;96(1):34–45. doi:10.1016/j.critrevonc.2015.04.011
36. Gornstein EL, Schwarz TL. Neurotoxic mechanisms of paclitaxel are local to the distal axon and independent of transport defects. *Exp Neurol*. 2017;288:153–166. doi:10.1016/j.expneurol.2016.11.015
37. Areti A, Yerra VG, Naidu V, Kumar A. Oxidative stress and nerve damage: role in chemotherapy induced peripheral neuropathy. *Redox Biol*. 2014;2:289–295. doi:10.1016/j.redox.2014.01.006
38. Siau C, Bennett GJ. Dysregulation of cellular calcium homeostasis in chemotherapy-evoked painful peripheral neuropathy. *Anesth Analg*. 2006;102(5):1485–1490. doi:10.1213/01.ane.0000204318.35194.ed
39. Zhang H, Dougherty PM. Enhanced excitability of primary sensory neurons and altered gene expression of neuronal ion channels in dorsal root ganglion in paclitaxel-induced peripheral neuropathy. *Anesthesiology*. 2014;120(6):1463–1475. doi:10.1097/ALN.0000000000000176
40. Staff NP, Fehrenbacher JC, Caillaud M, et al. Pathogenesis of paclitaxel-induced peripheral neuropathy: a current review of in vitro and in vivo findings using rodent and human model systems. *Exp Neurol*. 2020;324:113121. doi:10.1016/j.expneurol.2019.113121

## International Journal of Nanomedicine

Dovepress

### Publish your work in this journal

The International Journal of Nanomedicine is an international, peer-reviewed journal focusing on the application of nanotechnology in diagnostics, therapeutics, and drug delivery systems throughout the biomedical field. This journal is indexed on PubMed Central, MedLine, CAS, SciSearch®, Current Contents®/Clinical Medicine, Journal Citation Reports/Science Edition, EMBase, Scopus and the Elsevier Bibliographic databases. The manuscript management system is completely online and includes a very quick and fair peer-review system, which is all easy to use. Visit <http://www.dovepress.com/testimonials.php> to read real quotes from published authors.

Submit your manuscript here: <https://www.dovepress.com/international-journal-of-nanomedicine-journal>